

# Measurement of two-dimensional movement parameters of the carotid artery wall for early detection of arteriosclerosis: a preliminary clinical study

Guillaume Zahnd<sup>1</sup>, Loïc Boussel<sup>1,2</sup>, Adrien Marion<sup>1</sup>, Marion Durand<sup>3</sup>, Philippe Moulin<sup>3</sup>, André Sérusclat<sup>2</sup>, Didier Vray<sup>1</sup>

<sup>1</sup>Université de Lyon, CREATIS; CNRS UMR 5220; Inserm U1044; INSA-Lyon, France

<sup>2</sup>Department of Radiology; Louis Pradel Hospital, Lyon, France

<sup>3</sup>Department of Endocrinology; Louis Pradel Hospital, Lyon, France

*Manuscript published in *Ultrasound in Medicine & Biology*, vol. 37, no. 9, pp. 1421-1429, 2011, DOI: 10.1016/j.ultrasmedbio.2011.05.843.*

*The final version of the paper is available at:*

*<http://www.sciencedirect.com/science/article/pii/S0301562911011057>*

## Abstract

The aim of this study was to clinically investigate the association between the risk factors of early-stage atherosclerosis and the two-dimensional (2D) movement of the artery wall. To meet this objective, a speckle tracking approach for the estimation of the 2D trajectory of the vessel wall was proposed and applied to B-mode ultrasound (US) sequences of the left common carotid artery (CCA). A deformable skeleton model was also introduced in the block matching scheme. Finally, the 2D movements of both proximal and distal walls were investigated in three different local regions, with  $1.5 \times 0.3$  mm<sup>2</sup> kernel blocks. A clinical study was conducted in which two different populations (26 young healthy volunteers and 26 older diabetic patients) were studied. The results show that the mean amplitude value of the diameter change  $\Delta D$ , of the longitudinal displacement of the proximal wall  $\Delta X_p$ , and of the longitudinal displacement of the distal wall  $\Delta X_d$  were  $0.65 \pm 0.17$  vs  $0.41 \pm 0.12$  mm ( $p < 0.001$ ),  $0.48 \pm 0.21$  vs  $0.26 \pm 0.18$  mm ( $p < 0.001$ ), and  $0.48 \pm 0.20$  vs  $0.35 \pm 0.23$  mm ( $p = 0.006$ ) for the young healthy volunteers and the older diabetic patients respectively. The results of the three dynamic parameters  $\Delta D$ ,  $\Delta X_p$  and  $\Delta X_d$  were systematically and significantly lower for the diabetic subjects, respectively 37%, 46%, and 27%. The method introduced in this feasibility study might constitute a pertinent approach to assess the presence of early-stage arteriosclerosis by the noninvasive estimation of the 2D motion of the intima-media complex in the CCA.

**Keywords:** *2D motion estimation; Arteriosclerosis; Atherosclerosis; B-mode ultrasound; Carotid artery; Shear stress; Speckle tracking*

## Introduction and literature

Cardiovascular diseases (CVDs) are responsible for one-third of deaths throughout the world, and are the major cause of morbidity and mortality in most countries. Myocardial infarction and stroke are mostly triggered by the rupture of atheromatous plaques in arterial blood vessels at the final stage of the atherosclerosis process (Schaar et al, 2004). However, a study (Ford et al, 2007) has shown that from 1980 to 2000, the age-adjusted death rate for coronary heart disease dramatically decreased by more than half, and approximately 44% was attributed to changes in risk factors, *i.e.*, in preventive care. Furthermore, in the atherosclerosis process, significant changes of the mechanical properties of the vascular wall may occur before the anatomical changes of the intima-media thickness (IMT) become visible (Alva et al, 1993). Early detection of this pathology is therefore an important issue.

Prevention is based on the detection of at-risk patients from risk groups (such as tobacco smokers, diabetics, and patients with essential hypertension, end-stage renal disease, high cholesterol) or risk-factors. However, traditional risk factors may lead to false-positive or false-negative errors and often fail to predict major cardiovascular events and lead to treating millions of individuals whose risk is unknown (Helfand et al, 2009). Recent work has shown that artery stiffness is an independent predictor of CVD (Laurent et al, 2001), (Shokawa et al, 2005) and that carotid elasticity is correlated with an increasing number of risk factors (Okimoto et al, 2008). Thus, new markers of early arterial wall alteration have been developed, but their performance as screening tests remains poor (Simon et al, 2006). These markers focus on arterial wall thickness by measuring the IMT, on wall calcification by estimating the coronary artery calcium score (CAC), and on arterial wall stiffness by assessing the ankle-arm index pressure (AAI) and the pulse wave velocity (PWV). Information concerning the circulatory system can be provided by the wave intensity hemodynamic index (Niki et al, 2002). The Young modulus and the pressure strain elastic modulus that characterize vascular elasticity can be estimated by tissue Doppler imaging (TDI) (Claridge et al, 2008), (Kawasaki et al, 2009). Stiffness is also widely investigated in arterial imaging techniques using diameter changes of the vessel and blood pressure (Bjällmark et al, 2010).

Recent studies have also considered the longitudinal movement of the common carotid artery (CCA) wall with B-mode ultrasound imaging *in vivo* using a speckle tracking approach (Golemati et al, 2003) or an echo tracking approach (Persson et al, 2002), (Persson et al, 2003), (Cinthio et al, 2005), (Cinthio and Ahlgren, 2010). It has been shown that the arterial wall was subject to a reproducible two-dimensional (2D) motion, having similar radial and longitudinal amplitudes, *i.e.* of millimeter magnitude (Persson et al, 2002), (Persson et al, 2003), (Cinthio et al, 2006).

Block matching, also called speckle tracking in ultrasonic imaging, is a method that is widely used to estimate the 2D tissue motion through B-mode ultrasound image sequences (Yeung et al, 1998b), (Meunier, 1998), (Bohs et al, 2000). The block matching technique (Giachetti, 2000) is commonly applied locally to find the displacement of a block of pixels between two successive frames. Given a reference kernel block  $K$  in an original image, matching consists in finding the most similar

pattern in the next image. The size of the kernel must be well adapted to the dimensions of the tracked object. The search is computed inside a region of interest (ROI) that defines the maximum possible displacements to avoid incoherent movements and decrease computational complexity. The similarity criterion used in this study is the sum of squared differences (SSD) (Viola and Walker, 2003), and can be defined as:

$$SSD(x, y, t) = \sum_x \sum_y (\mathbf{I}(x, y, t) - \mathbf{I}(x + dx, y + dy, t + dt))^2, \quad (1)$$

where  $\mathbf{I}(x, y, t)$  is the image intensity value at position  $(x, y)$  and at time  $t$ . The displacement  $\mathbf{d}$  that corresponds to the optimal block position in the next image is found by minimizing the function:

$$\mathbf{d}(x, y) = \operatorname{argmin}(SSD(x, y, t)), \quad (2)$$

The aim of this study was to estimate noninvasively the 2D motion of the intima-media complex in the CCA, and to compare several motion parameters between two different populations of young healthy volunteers and older diabetic subjects. Our approach is based on our own specific time-domain speckle tracking method, called CAROLAB. This paper is organized as follows. Section 2 describes the material and methods. The study population and the acquisition protocol are presented first. Then the speckle tracking algorithm is described and the motion parameters considered are detailed. Finally, the reproducibility study and the statistical analysis are presented. Section 3 presents the results, which are discussed in Section 4. Finally, conclusions and perspectives are given in Section 5.

## Materials and Method

### Subjects

Diabetes has been reported to be a precursor for cardiovascular mortality and morbidity (Kannel and McGee, 1979). Twenty-six young healthy volunteers and 26 older diabetic patients were involved in this study. The healthy volunteers were 10 males and 16 females, aged from 19 to 54 years (mean age =  $25.7 \pm 9.0$  years). The diabetic patients were 16 males and 10 females aged from 39 to 73 years (mean age =  $57.7 \pm 9.2$  years). The inclusion criterion for the diabetic patients was type 1 or 2 diabetes diagnosed at least 1 year before. No other criterion, including clinical characteristics, was used to select these subjects. Healthy volunteers were cardiovascular risk factor-free (tobacco use, hypercholesterolemia, diabetes, hypertension or particular family history) as assessed by an oral questionnaire. Informed consent was obtained from all participants. The study was conducted in compliance with the requirements of our institutional review board and the ethics committee.

### Collection of ultrasound sequences of the common carotid artery

All investigations were conducted at Louis Pradel Hospital, Lyon, France, by a single medical doctor. Ultrasound imaging was processed with a medical scanner (Antares,

Siemens Erlangen), equipped with a 7.5– to 10–MHz linear array transducer. Longitudinal B-mode image sequences of the left CCA were acquired for all subjects. After a rest in the supine position in a quiet room 15 min before examination, the subjects were examined in the supine position with the neck extended and rotated 45° to the contralateral side. The transducer was centered on the common carotid artery, 2 cm proximal to the carotid bifurcation in the longitudinal plane. The absence of focal atherosclerosis plaques in the imaged area was assessed by the medical doctor. The B-mode sequence frame rate was 26 fps, each frame covering a 17–mm–deep and 23–mm–wide region. Images were recorded through at least two cardiac cycles. The influence of respiration have been investigated in (Cinthio et al, 2005), and it has been shown that the movement due to breathing superimpose to the longitudinal movement due to the cardiac cycle. In order to avoid the influence of the movement due to breathing, all the acquisitions have been performed with the subjects suspending their respiration. The focal point was positioned on the lumen-intima interface of the distal wall. The pixel dimensions of B-mode images were 30  $\mu\text{m}$  in both radial and longitudinal directions. The dynamic range was set to 65 dB. These instrumentation settings were maintained for all follow-up examinations. In all studies, the blood pressure was measured at the subject’s arm and the electrocardiogram was monitored. All sequences were stored digitally and transferred to a commercial computer for further image analysis. No subject have been rejected from the study. The IMT of the distal wall has been manually measured on the first image of each sequence by a medical doctor. Figures 2 and 3, respectively, show a healthy carotid (22 year-old female) with a high image quality, and a pathological carotid (64 year-old male, type 2 diabetes) with a lower image quality.

## Block matching algorithm

For this study, software called CAROLAB was developed in Matlab (2009b, The MathWorks, Inc., Natick, MA, USA) to assist medical doctors in experimental data processing. CAROLAB is used to load and visualize Dicom sequences, position the kernel blocks on desired regions, process the speckle tracking algorithm, visualize the displacement of the kernels throughout the sequence, and then save and export the results.

The 2D movement of both proximal and distal walls of the CCA is investigated in each sequence. We considered three local regions along the artery (Figure 4). Indeed, to prevent the degrading phenomena inherent to ultrasound imaging (such as occlusions, weak echoes, movement artifacts, and out-of-plane movement) that may introduce error in the motion estimation, the 2D movement was assessed at three different regions of the CCA wall. Each local region comprised a set of two radially opposed ROIs and their corresponding kernel (Figure 4). The kernel  $K_p$  was positioned in the intima-media complex of the proximal wall, and the kernel  $K_d$  was positioned at the opposite side of the artery, in the intima-media complex of the distal wall (Figure 4). Each kernel measured  $1.5 \times 0.3 \text{ mm}^2$ . Particular care was taken to position each local region on a distinct and contrasted echo of an inhomogeneity or irregularity, in order to benefit from a discernible pattern for speckle tracking. The performance of tracking was evaluated by two medical experts by visually verifying the displacement of each block by replaying the sequence. The set of two kernels  $K_p$  and  $K_d$  from the same local region

with the best tracking accuracy as evaluated visually were chosen.

Previous studies (Cinthio et al, 2005) have shown that the displacement amplitude of the intima-media complex was approximately 1 mm in both radial and longitudinal directions for a healthy adult. Given a spatial quantification of  $30 \mu\text{m}/\text{pixel}$  provided by the ultrasound scanner, the movement is described by a total amplitude of approximately 33 pixels in both directions, and the displacement between two consecutive images is often just a few pixels. In order to obtain a finer resolution of the motion estimation during the cardiac cycle, the ROI was interpolated by a factor of 10. The interpolation was bilinear and achieved with the Matlab (2009b, The MathWorks, Inc., Natick, MA, USA) function `interp2`. However, for the sake of computational complexity, we introduced a double-step interpolation scheme (Figure 5). Firstly, the coarse displacement  $\mathbf{d}_1$  of the kernel in the standard ROI was estimated without interpolation. Secondly, a smaller ROI that is only one pixel larger than the kernel on each side is centered on the coarse position and interpolated. The residual subpixelic displacement  $\mathbf{d}_2$  is then estimated. Finally, the total fine displacement  $\mathbf{d}$  corresponds to the sum of the two displacements  $\mathbf{d}_1$  and  $\mathbf{d}_2$ .

The robustness of the speckle tracking algorithm can be increased using a deformable mesh (Yeung et al, 1998a). Given that the structure of the CCA is mainly longitudinally rectilinear, we introduce here a specific linear skeleton model composed of five nodes  $N_i$  ( $i=1..5$ ) aligned longitudinally (Figure 6), which fits the morphological structure of the CCA (Figure 1). Each node is the center of a kernel block  $K$  described previously, and the distance between two nodes is equal to half of the kernel width. The central node  $N_3$  represents the position of the considered block. The four peripheral nodes  $N_1, N_2, N_4, N_5$ , are automatically positioned in reference to the central node and are used to adjust the position of the central node after the block matching operation. The position  $\tilde{N}(x, y)$  of the central node after the block matching is calculated by averaging the position of the five nodes  $N_i$  ( $i=1..5$ ). Figure 6 shows the proposed deformable scheme. After each iteration, the five nodes are lined up again around the position of the considered block.

Finally, the motion of the kernel estimated with the speckle tracking method is used in each frame to translate the ROI, until the end of the sequence. Two medical experts visualized the sequences with the resulting displacement of the blocks and evaluated the quality of the tracking for each kernel. The pair of proximal and distal kernels with the highest fidelity to the image movement was chosen. In a few cases, none of the three results was satisfactory and the speckle tracking was processed one more time with a different initial blocks position, so every subject was included in the study.

## Measurement of the wall movement

This study considered several movement parameters that were all derived from the wall 2D trajectory estimated by the speckle tracking algorithm. Both proximal and distal walls were investigated with the kernels  $K_p$  and  $K_d$ , respectively. The 2D coordinates of a kernel block along a sequence are defined by the successive longitudinal and radial positions  $[\mathbf{X}(t), \mathbf{Y}(t)]$  of its center, relative to the upper left corner of the image. The parameter  $\Delta D$  corresponds to the maximum amplitude of the lumen diameter change

during one cardiac cycle:

$$\Delta D = D(t)_{max} - D(t)_{min}, \quad (3)$$

with  $D(t)$  the lumen diameter, corresponding to the radial distance between the kernels  $K_p$  and  $K_d$ :

$$D(t) = |Y_p(t) - Y_d(t)|. \quad (4)$$

The parameters  $\Delta X_p$  and  $\Delta X_d$  correspond to the maximum longitudinal amplitude of the displacements  $X(t)$  of the proximal and distal wall, respectively, during one cardiac cycle:

$$\Delta X_p = X_p(t)_{max} - X_p(t)_{min} \quad (5)$$

$$\Delta X_d = X_d(t)_{max} - X_d(t)_{min} \quad (6)$$

## Statistical analysis

The Mann–Whitney U test was used to compare the values of radial, longitudinal proximal and longitudinal distal displacement of young healthy volunteers and older diabetic patients. Intra- and inter-reader reproducibility was evaluated on 16 randomly selected subjects (eight healthy volunteers and eight diabetic patients). Measurements of radial, proximal longitudinal, and distal longitudinal displacement were taken twice by the same operator (intra-reader) and once by another operator (inter-reader) from the same acquired ultrasound sequence. The measurement errors  $err$  were then calculated as below:

$$err = 100 \times \frac{\sqrt{var}}{m}, \quad (7)$$

with  $var$  the within-subject variance and  $m$  the average of all measurements (Martin Bland and Altman, 1986). To determine the level of intra- and inter-reader agreement between two repeated measurements, the intraclass correlation coefficient (ICC) with its 95% confidence interval (CI) was also calculated. The value  $p \leq 0.05$  was considered to indicate a statistically significant difference. All statistical analyses were performed using Intercooled Stata 10.0 (StataCorp LP, College Station, TX, USA).

## Results

The study was conducted on two different populations (26 young healthy volunteers and 26 older diabetic patients). For each subject, the amplitude of the diameter change  $\Delta D$  and of the longitudinal motion of the proximal and distal wall  $\Delta X_p$  and  $\Delta X_d$ , respectively, was estimated by the method described in Section 2.

Figure 7 shows the diameter change and the longitudinal movement of the CCA for one healthy volunteer (22 year-old female) and one diabetic patient (64 year-old male, type 2 diabetes), corresponding to the B-mode images presented in Figures 2 and 3 respectively. The two sequences are approximately 3 s long (75 frames) and cover more than two cardiac cycles.

For both study populations, the mean amplitude, the standard deviation (SD) and the range corresponding to the IMT and the 2D movement parameters of the artery wall are detailed in Table 1, with the corresponding p-values.

The differences between the two groups were statistically significant for all the three parameters on the Mann–Whitney U tests ( $p < 0.001$ ,  $p < 0.001$ ,  $p = 0.006$ ) (Figure 8).

Intraobserver measurement errors for the radial, proximal, and distal longitudinal displacement were 9.9%, 21.5%, and 18.6%, respectively. Similarly, interobserver measurement errors were 15.7%, 14.4%, and 21.9%, respectively. The intraobserver ICCs were 0.92 (95% CI=0.79–0.97), 0.90 (95% CI=0.75–0.87), and 0.86 (95% CI=0.65–0.95). The interobserver ICCs were 0.92 (95% CI=0.78–0.97), 0.97 (95% CI=0.92–0.98), and 0.88 (95% CI=0.69–0.95).

## Discussion and Summary

The carotid artery wall is subject to a two-dimensional movement throughout the cardiac cycle, with both radial and longitudinal components of the magnitude millimeter (Cinthio et al, 2005). This study introduces a method based on speckle tracking dedicated to estimate *in vivo* the 2D trajectory of selected points of the wall.

This study, designed as a proof of concept, investigated two extremely different populations (26 young healthy volunteers and 26 older diabetic patients with high atherosclerosis risk and likely to present arteriosclerosis). The major contribution of this study is the ability to estimate and compare the amplitude of three movement parameters (Table 1), introduced in Section 2. The results were significantly different between the two populations (Figure 8). The mean results of the older diabetic patients compared to the young healthy subjects were systematically and significantly lower for the three parameters considered: 37%, 46% and 27% for  $\Delta D$ ,  $\Delta X_p$ , and  $\Delta X_d$  respectively. This difference of behavior clearly shows the effect of the arteriosclerotic process on the artery walls.

This study was conducted in clinical conditions, and a substantial number of subjects were studied (N=52), a strong point in this investigation. Among the acquired data, some B-mode sequences of the CCA suffered from poor image quality, especially images of pathological subjects' CCA. An image was declared to have a poor quality when the typical double-line pattern of the wall (Figure 1) could not be seen and the images had a low signal-to-noise ratio (SNR). In this study, we assume that the real tissue displacements corresponds to the estimated translations of the speckle patterns with the hypothesis of speckle conservation (Yeung et al, 1998a). In a few cases, the tracking of the blocks was erroneous on the images with the lower quality, *i.e.* the visual control showed that the blocks did not follow the tissue movement. In these cases, the medical doctor had thus to process the tracking again with another initial block position, and each subject have been included in the study.

Recent studies applied to the carotid artery proposed an optimal kernel size (Golemati et al, 2003) of  $3.2 \times 2.5 \text{ mm}^2$ . However, such a large kernel covers almost the entire intima-media complex and includes approximately 1.2 mm of the lumen. Hence the average movement of the kernel does not precisely correspond to the motion of the different layers of tissues considered. Other studies (Cinthio et al, 2005) introduced an echo tracking approach that uses a very small kernel size, approximately  $0.1 \times 0.1 \text{ mm}^2$ , corresponding to two square pixels. This method has several prerequisites regarding image quality: the double-line pattern from the boundaries of the lumen-intima and media-adventitia (Figure 1) must be clearly visible at the proximal and distal walls, and

the preselected distinct echo of an inhomogeneity or an irregularity must be visible in all the images over several cardiac cycles (Cinthio et al, 2006). This method may not be adapted to a large medical study, where carotid imaging often suffers from poor quality, especially in the case of pathological subjects. In our work, we propose an intermediate kernel size of  $1.5 \times 0.3 \text{ mm}^2$ , which is included inside the intima-media complex. The use of kernel blocks with an important width and a low height is designed to cover a large surface of the intima-media complex, without covering the adventitia layer or the lumen.

In the longitudinal direction, the speckle pattern of the tracked region does not always present an important contrast that allow to distinguish precisely a block from its immediate neighbors. In order to gain longitudinal accuracy with the speckle tracking method, we use wider blocks to increase the differences in the pattern. Our method estimates the global displacement of the whole intima-media complex rather than the local displacement of a point. Nevertheless, a wide kernel does not allow the same accuracy when tracking a point because the trajectory is governed by the behavior of all the pixels in a wider zone. Since the absence of focal atherosclerosis plaques in the imaged area has been assessed by the medical doctor, we use the hypothesis that the difference between the 2D motion of two points of the same wall is negligible at our framerate. Moreover, each initial kernel was the center of a deformable skeleton mesh (Figure 6) composed of five longitudinally aligned blocks. The skeleton covers a wider area ( $4.5 \times 0.3 \text{ mm}^2$ ) of the layers and reflects a more global behavior of the wall. The displacement of the skeleton was averaged and used to translate the kernel block. The major problem of the absence of a gold standard to control the accuracy of the measurements remains. The tracking quality was evaluated by two medical doctors by visually controlling that the displacement of the kernel blocks corresponded precisely to the movement of the tissues.

One drawback of our approach is that it is user-dependent. Firstly, the kernel blocks were manually positioned by a medical expert in the initial image of the sequence. Particular care must be taken so that each initial point corresponds to a local visible distinct echo of an inhomogeneity or an irregularity inside the intima-media complex. Furthermore, the kernels were preferably placed in local regions where the vessel was rectilinear and horizontal. Secondly, the trajectory of each block must be visually verified through the result sequence, and the pair of kernels  $K_p$  and  $K_d$  having the best tracking accuracy is chosen. However, the reproducibility study showed satisfactory results for inter- and intraobserver measurements, both with an ICC value of 0.92.

In our study, the longitudinal displacement of the arterial wall is of large amplitude (up to 1 mm). This is in accordance with the findings of (Cinthio et al, 2006) who reported that the longitudinal movement is comparable to the radial displacement and significantly contributes to the arterial wall displacement. It also corroborates the findings of (Warriner et al, 2008) who proposed a realistic viscoelastic model of the vessel based on the hemodynamics and the wall physiology. The global pattern of the wall motion is indeed complex, involving several phenomena including the pulse wave, the longitudinal tension and the elastic recoil of the arterial wall.

The wall shear stress is the force per unit area created when the tangential force of the blood flow acts on the surface of the endothelium (Davies, 2008). In addition to

thickness and stiffness, shear stress is an important determinant in arterial wall pathophysiology (Malek et al, 1999), as it can affect the endothelial function and is a factor in the development of atherosclerosis (Cunningham and Gotlieb, 2004), (Slager et al, 2005), (Groen et al, 2007), (Chatzizisis et al, 2007). However, the exact influence of the shear stress on the arterial wall longitudinal movement is unknown and other contribution forces, possibly of major importance, may also be present (Nilsson et al, 2009). Furthermore, this single phenomenon does not explain the triphasic movement pattern with a larger movement against the blood flow during systole described in (Cinthio et al, 2005) and (Cinthio et al, 2006).

A limitation of our study is the absence of measurement of the movement within the wall, *i.e.* the shear strain induced between the different layers of the carotid artery. This important parameter reported by several teams (Cinthio et al, 2006), (Hodis and Zamir, 2008) is reflecting the wall stiffness. Nevertheless, the global 2D movement resulting from the elastic shift deformation of the wall layers (Persson et al, 2002), (Persson et al, 2003), (Golematis et al, 2003), (Cinthio et al, 2005), (Cinthio and Ahlgren, 2010) estimated according to the method we propose is closely related to wall elasticity.

## Conclusion

We introduced a speckle tracking method dedicated to the estimation of several 2D movement parameters of the vessel wall. A preliminary clinical study was conducted and a significant amplitude difference was found between the young healthy and the older pathological populations. Risk factors were found to be correlated with the 2D movement amplitude of the vessel. Our approach clearly shows the distinct contribution of the longitudinal motion to the artery behavior, and could constitute an additional marker of early arterial wall abnormalities leading to premature arteriosclerosis. The assessment of additional mechanical parameters, such as shear stress, would provide a better characterization of the vessel. Further validation will be tested in larger clinical studies.

## Figures

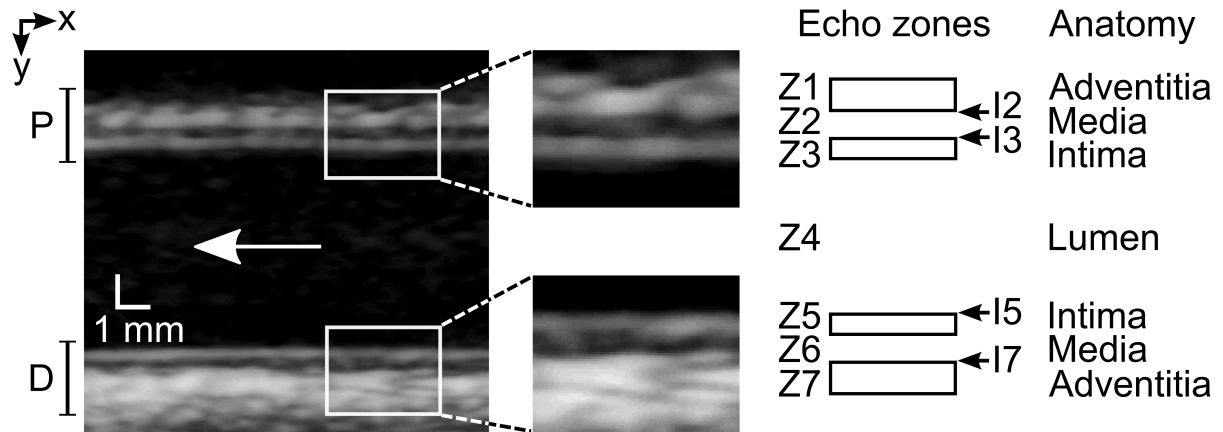


Figure 1: Longitudinal B-mode image of a common carotid artery (CCA). The different echo zones correspond to the three concentric layers, *i.e.*, adventitia, media, and intima. *P* and *D* stand for the proximal wall and the distal wall, respectively. The white arrow represents the blood flow direction.

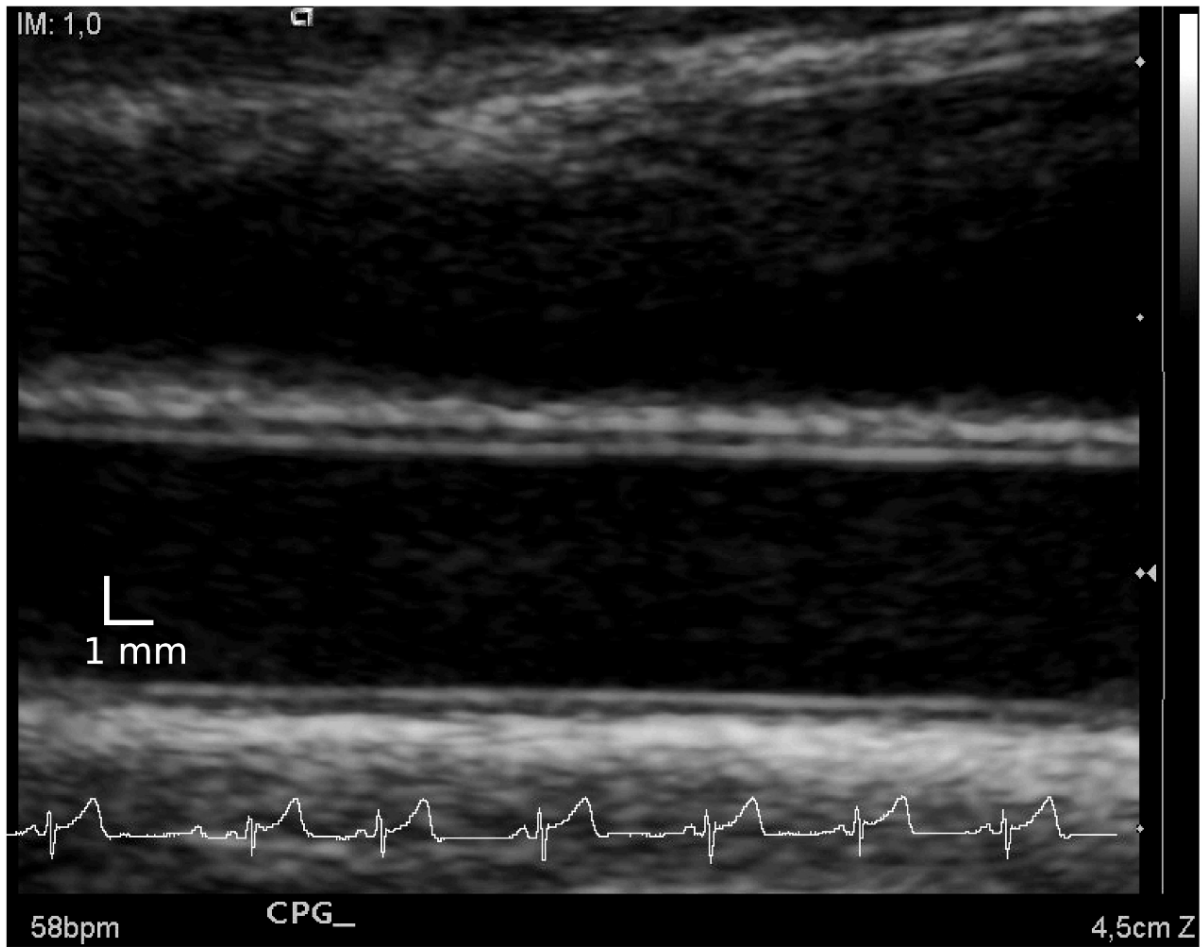


Figure 2: Longitudinal B-mode image of a healthy common carotid artery (CCA). The intima-media thickness (IMT) is 520  $\mu\text{m}$ .

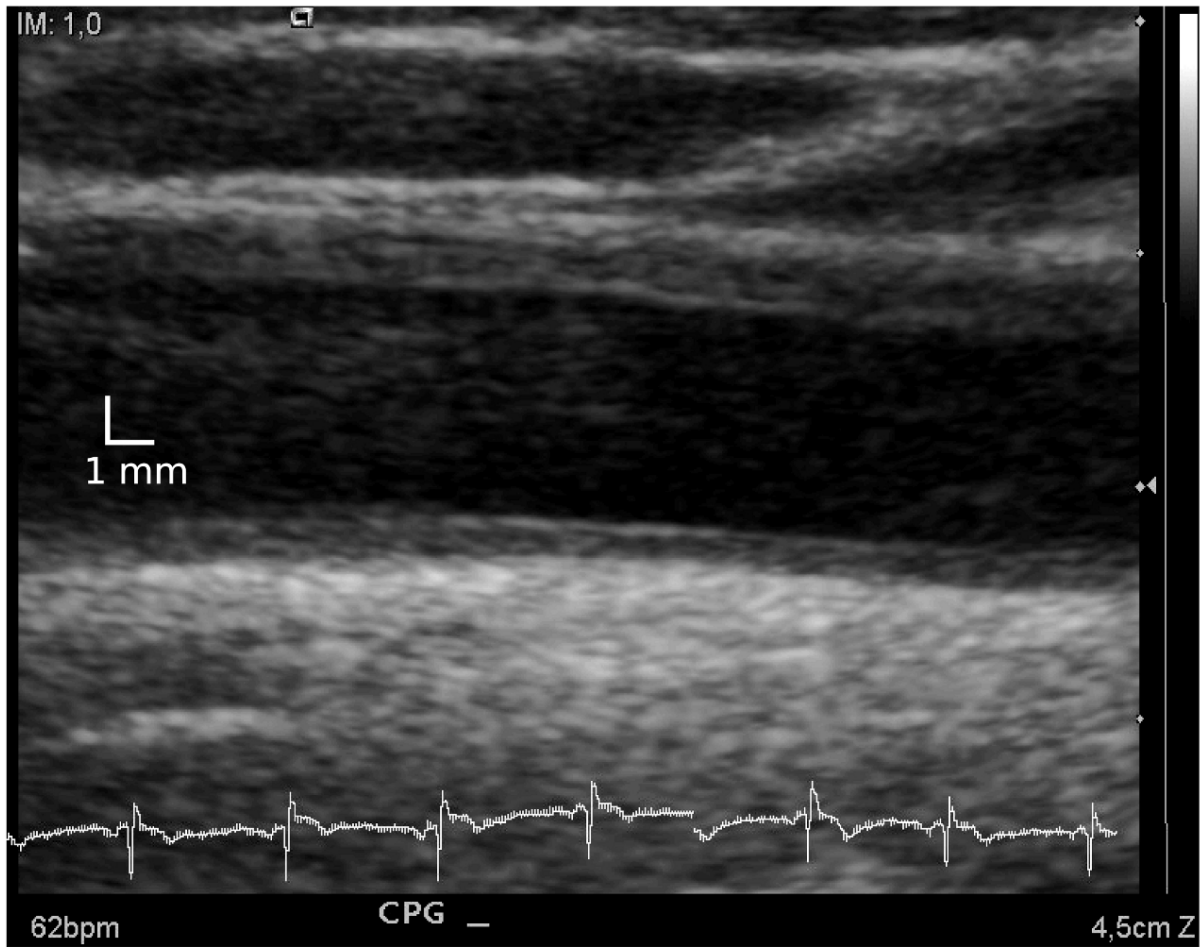


Figure 3: Longitudinal B-mode image of a pathological (type 2 diabetes) common carotid artery (CCA). The intima-media thickness (IMT) is 850  $\mu\text{m}$ .

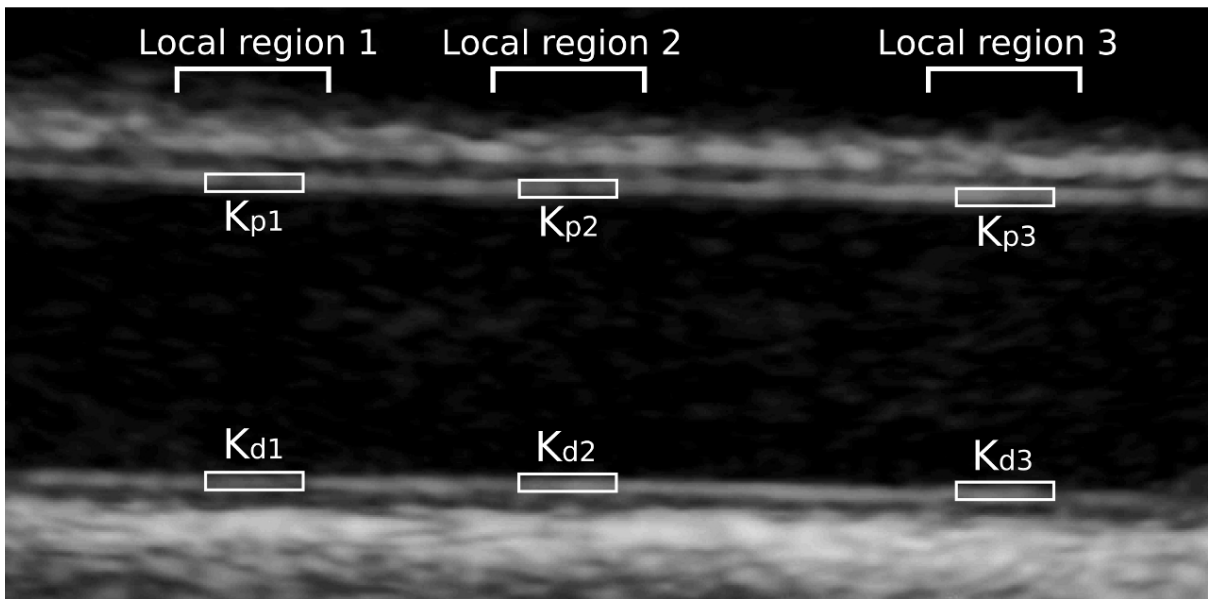


Figure 4: Position of the kernel blocks  $K_p$  and  $K_d$  in the proximal and the distal wall, respectively, in three different local regions.

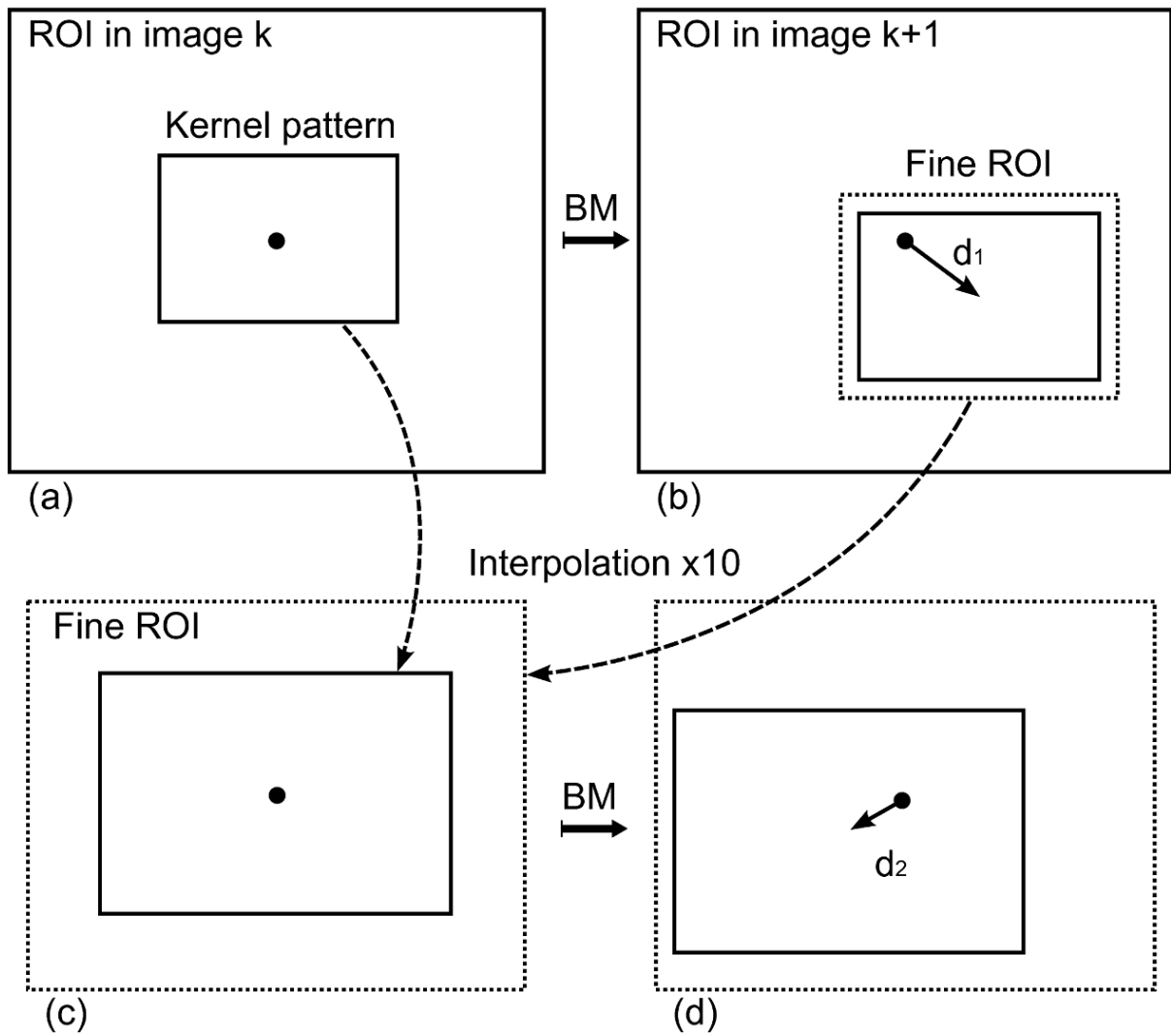


Figure 5: Double-step interpolation scheme. (a) The kernel is first positioned at the center of the region of interest (ROI) in the image  $k$ . (b) The coarse displacement  $\mathbf{d}_1$  is estimated by the block matching (BM) method, then the fine ROI, just one pixel larger than the kernel, is set in the image  $k+1$ . (c) The original kernel and the fine ROI are both interpolated by a factor of 10. (d) The fine residual displacement  $\mathbf{d}_2$  is estimated in the fine ROI using the block matching method.

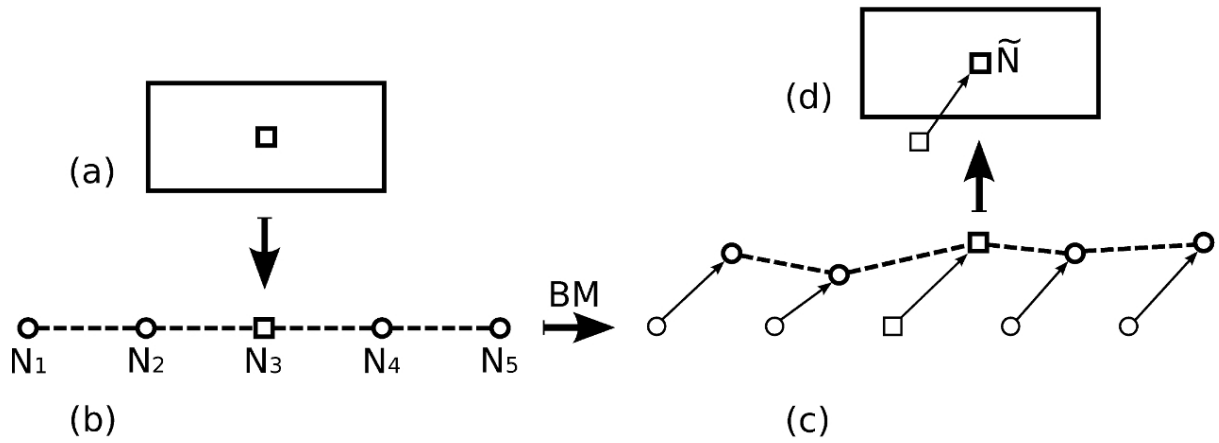


Figure 6: Deformable linear skeleton model. (a) Original kernel block and its center (square) in the image  $k$ . (b) Generation of the skeleton: the central node  $N_3$  corresponds to the position of the center of the kernel. (c) The block matching (BM) method is applied to the five kernels centered on the nodes and five displacements are estimated. (d) The position  $\tilde{N}(x, y)$  of the kernel in the image  $k+1$  is estimated from the mean displacement of the five nodes.

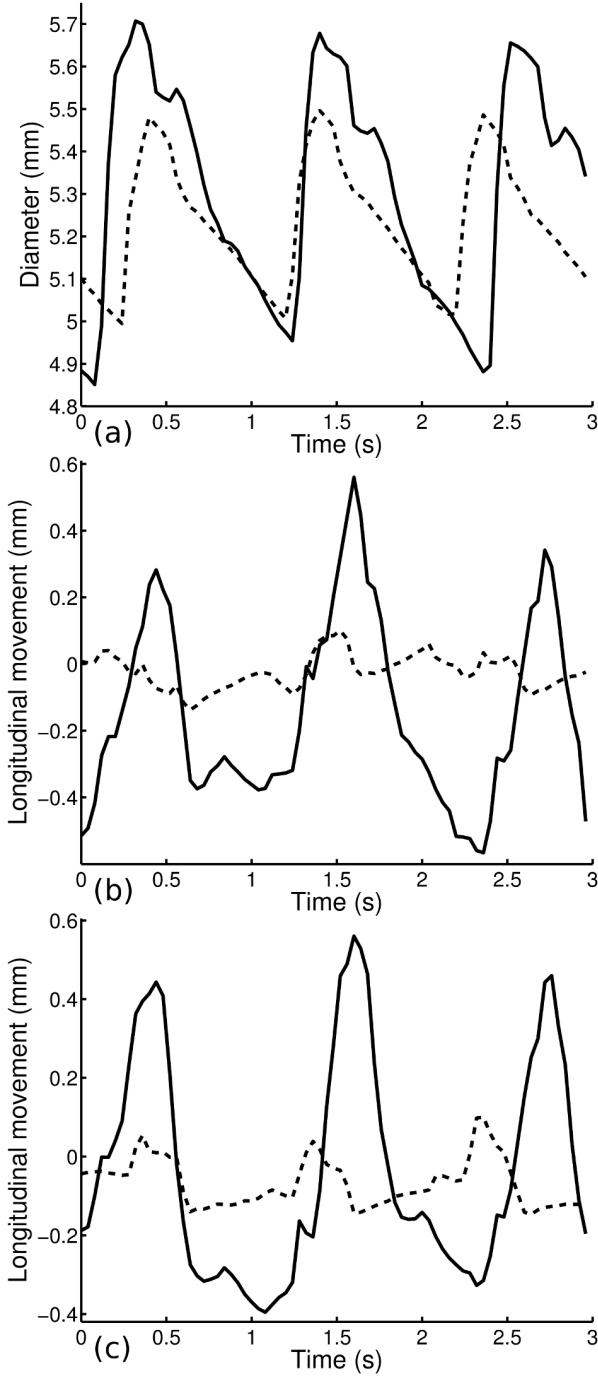


Figure 7: Trajectory of a healthy carotid (22 year-old female, solid line) and a pathological carotid (64 year-old male diabetic patient, dashed line). (a) Diameter change  $D(t)$ : the amplitude of the diameter change  $\Delta D$  and the compliance  $\Delta D/D(t)_{min}$  are, respectively, 0.775 mm and 15.9% for the healthy carotid and 0.477 mm and 9.5% for the pathological carotid. (b) Longitudinal movement of the proximal wall  $X_p(t)$ : the amplitude  $\Delta X_p$  is 0.923 mm for the healthy carotid and 0.165 mm for the pathological carotid. (c) Longitudinal movement of the distal wall  $X_d(t)$ : the amplitude  $\Delta X_d$  is 0.871 mm for the healthy carotid and 0.211 mm for the pathological carotid.

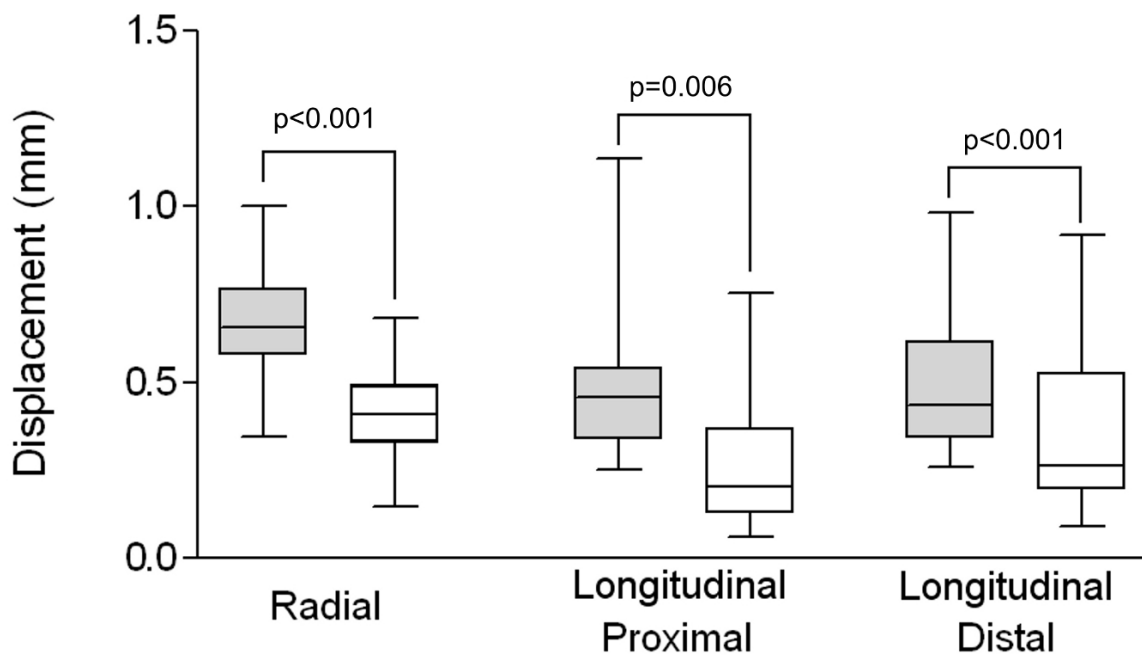


Figure 8: Box and whisker plots of radial, proximal longitudinal, and distal longitudinal displacement for healthy volunteers (gray boxes) and diabetic patients (white boxes). The boxes show the 25th and 75th percentile (interquartile) ranges. Median values (successively 0.65, 0.40, 0.45, 0.20, 0.43, 0.26 mm) are shown as a horizontal black bar within each box. The whiskers show levels outside the 5th and 95th percentiles ( $p=0.029$ ). The results of each Mann–Whitney U tests are expressed as p-values above the boxes.

## Table captions

**Table 1** Mean value, standard deviation and p-value for the intima-media thickness (IMT) and the three considered motion parameters: amplitude of the diameter change  $\Delta D$ , amplitude of the longitudinal movement of the proximal wall  $\Delta X_p$ , and of the longitudinal movement of the distal wall  $\Delta X_d$ , in control subjects and diabetic patients.

	26 young healthy volunteers		26 older diabetic patients		p value
	Mean values $\pm$ SD (mm)	Range (mm)	Mean values $\pm$ SD (mm)	Range (mm)	
<i>IMT</i>	0.54 $\pm$ 0.08	0.43 - 0.73	0.82 $\pm$ 0.20	0.52 - 1.45	P<0.001
$\Delta D$	0.65 $\pm$ 0.17	0.33 - 1.07	0.41 $\pm$ 0.12	0.08 - 0.68	p<0.001
$\Delta X_p$	0.48 $\pm$ 0.21	0.23 - 1.34	0.26 $\pm$ 0.18	0.03 - 0.77	p<0.001
$\Delta X_d$	0.48 $\pm$ 0.20	0.25 - 1.08	0.35 $\pm$ 0.23	0.08 - 1.02	p=0.006

## References

- Alva F, Samaniego V, Gonzalez V, Moguel R, Meaney E. Structural and dynamic changes in the elastic arteries due to arterial hypertension and hypercholesterolemia. *Clinical cardiology*. 1993;16(8):614–618.
- Bjällmark A, Lind B, Peolsson M, Shahgaldi K, Brodin L, Nowak J. Ultrasonographic strain imaging is superior to conventional non-invasive measures of vascular stiffness in the detection of age-dependent differences in the mechanical properties of the common carotid artery. *European Journal of Echocardiography*. 2010;11(7):630–636.
- Bohs L, Geiman B, Anderson M, Gebhart S, Trahey G. Speckle tracking for multi-dimensional flow estimation. *Ultrasonics*. 2000;38(1-8):369–375.
- Chatzizisis Y, Coskun A, Jonas M, Edelman E, Feldman C, Stone P. Role of Endothelial Shear Stress in the Natural History of Coronary Atherosclerosis and Vascular Remodeling: Molecular, Cellular, and Vascular Behavior. *Journal of the American College of Cardiology*. 2007;49(25):2379–2393.
- Cinthio M, Ahlgren Å. Intra-observer variability of longitudinal displacement and intramural shear strain measurements of the arterial wall using ultrasound noninvasively in vivo. *Ultrasound in Medicine & Biology*. 2010;36(5):697–704.
- Cinthio M, Ahlgren Å, Bergkvist J, Jansson T, Persson H, Lindström K. Longitudinal movements and resulting shear strain of the arterial wall. *American Journal of Physiology- Heart and Circulatory Physiology*. 2006;291(1):H394.
- Cinthio M, Ahlgren Å, Jansson T, Eriksson A, Persson H, Lindström K. Evaluation of an ultrasonic echo-tracking method for measurements of arterial wall movements in two dimensions. *IEEE Transactions on Ultrasonics, Ferroelectrics, and Frequency Control*. 2005;52(8):1300–1311.
- Claridge M, Bate G, Dineley J, Hoskins P, Marshall T, Adam D, Bradbury A, Wilkink A. A Reproducibility Study of a TDI-Based Method to Calculate Indices of Arterial Stiffness. *Ultrasound in Medicine & Biology*. 2008;34(2):215–220.
- Cunningham K, Gotlieb A. The role of shear stress in the pathogenesis of atherosclerosis. *Laboratory investigation*. 2004;85(1):9–23.
- Davies P. Hemodynamic shear stress and the endothelium in cardiovascular pathophysiology. *Nature Clinical Practice Cardiovascular Medicine*. 2008;6(1):16–26.
- Ford E, Ajani U, Croft J, Critchley J, Labarthe D, Kottke T, Giles W, Capewell S. Explaining the decrease in US deaths from coronary disease, 1980-2000. *The New England journal of medicine*. 2007;356(23):2388–2398.
- Giachetti A. Matching techniques to compute image motion. *Image and Vision Computing*. 2000;18(3):247–260.
- Golemati S, Sassano A, Lever M, Bharath A, Dhanjil S, Nicolaides A. Carotid artery wall motion estimated from B-mode ultrasound using region tracking and block matching. *Ultrasound in Medicine & Biology*. 2003;29(3):387–399.

- Groen H, Gijzen F, van der Lugt A, Ferguson M, Hatsukami T, van der Steen A, Yuan C, Wentzel J. Plaque rupture in the carotid artery is localized at the high shear stress region: a case report. *Stroke*. 2007;38(8):2379–2381.
- Helfand M, Buckley D, Freeman M, Fu R, Rogers K, Fleming C, Humphrey L. Emerging risk factors for coronary heart disease: a summary of systematic reviews conducted for the US Preventive Services Task Force. *Annals of internal medicine*. 2009;151(7):496–507.
- Hodis S, Zamir M. Solutions of the Maxwell viscoelastic equations for displacement and stress distributions within the arterial wall. *Physical Review E*. 2008;78(2):21914–1–21914–8.
- Kannel W, McGee D. Diabetes and cardiovascular risk factors: the Framingham study. *Circulation*. 1979;59(1):8–13.
- Kawasaki T, Fukuda S, Shimada K, Maeda K, Yoshida K, Sunada H, Inanami H, Tanaka H, Jissho S, Taguchi H, Yoshiyama M, Yoshikawa J. Direct Measurement of Wall Stiffness for Carotid Arteries by Ultrasound Strain Imaging. *Journal of the American Society of Echocardiography*. 2009;22(2):1389–1395.
- Laurent S, Boutouyrie P, Asmar R, Gautier I, Laloux B, Guize L, Ducimetiere P, Benetos A. Aortic stiffness is an independent predictor of all-cause and cardiovascular mortality in hypertensive patients. *Hypertension*. 2001;37(5):1236–1241.
- Malek A, Alper S, Izumo S. Hemodynamic shear stress and its role in atherosclerosis. *JAMA*. 1999;282(21):2035–2042.
- Martin Bland J, Altman D. Statistical methods for assessing agreement between two methods of clinical measurement. *The Lancet*. 1986;327(8476):307–310.
- Meunier J. Tissue motion assessment from 3D echographic speckle tracking. *Physics in Medicine and biology*. 1998;43:1241–1254.
- Niki K, Sugawara M, Chang D, Harada A, Okada T, Sakai R, Uchida K, Tanaka R, Mumford C. A new noninvasive measurement system for wave intensity: evaluation of carotid arterial wave intensity and reproducibility. *Heart and vessels*. 2002;17(1):12–21.
- Nilsson T, Ricci S, Ahlgren Å, Jansson T, Lindström K, Tortoli P, Persson H, Cinthio M. Methods for measurements of the longitudinal movement and the shear-induced longitudinal elastic modulus of the arterial wall. In: Yuh DP (Ed.), *Ultrasonics Symposium (IUS), 2009 IEEE International*. IEEE, IEEE, Piscataway, USA. 2009. pp. 317–320.
- Okimoto H, Ishigaki Y, Koiwa Y, Hinokio Y, Ogihara T, Suzuki S, Katagiri H, Ohkubo T, Hasegawa H, Kanai H, Oka Y. A novel method for evaluating human carotid artery elasticity: Possible detection of early stage atherosclerosis in subjects with type 2 diabetes. *Atherosclerosis*. 2008;196(1):391–397.
- Persson M, Ahlgren Å, Eriksson A, Jansson T, Persson H, Lindström K. Non-invasive measurement of arterial longitudinal movement. In: *IEEE Ultrasonics Symposium, 2002. Proceedings*. IEEE. 2002. Vol. 2, pp. 1783–1786.

- Persson M, Ahlgren Å, Jansson T, Eriksson A, Persson H, Lindström K. A new non-invasive ultrasonic method for simultaneous measurements of longitudinal and radial arterial wall movements: first in vivo trial. *Clinical physiology and functional imaging*. 2003;23(5):247–251.
- Schaar J, Muller J, Falk E, Virmani R, Fuster V, Serruys P, Colombo A, Stefanadis C, Ward C, Moreno P, Maseri A, van der Steen A. Terminology for high-risk and vulnerable coronary artery plaques. Report of a meeting on the vulnerable plaque, June 17 and 18, 2003, Santorini, Greece. *European heart journal*. 2004;25(12):1077–1082.
- Shokawa T, Imazu M, Yamamoto H, Toyofuku M, Tasaki N, Okimoto T, Yamane K, Kohno N. Pulse wave velocity predicts cardiovascular mortality: findings from the Hawaii-Los Angeles-Hiroshima study. *Circulation Journal*. 2005;69(3):259–264.
- Simon A, Chironi G, Levenson J. Performance of subclinical arterial disease detection as a screening test for coronary heart disease. *Hypertension*. 2006;48(3):392–396.
- Slager C, Wentzel J, Gijzen F, Schuurbiens J, van der Wal A, Van der Steen A, Serruys P. The role of shear stress in the generation of rupture-prone vulnerable plaques. *Nature Clinical Practice Cardiovascular Medicine*. 2005;2(8):401–407.
- Viola F, Walker W. A comparison of the performance of time-delay estimators in medical ultrasound. *IEEE Transactions on Ultrasonics, Ferroelectrics and Frequency Control*. 2003;50(4):392–401.
- Warriner R, Johnston K, Cobbold R. A viscoelastic model of arterial wall motion in pulsatile flow: implications for Doppler ultrasound clutter assessment. *Physiological Measurement*. 2008;29:157–179.
- Yeung F, Levinson S, Fu D, Parker K. Feature-adaptive motion tracking of ultrasound image sequences using a deformable mesh. *IEEE Transactions on Medical Imaging*. 1998a;17(6):945–956.
- Yeung F, Levinson S, Parker K. Multilevel and motion model-based ultrasonic speckle tracking algorithms. *Ultrasound in Medicine & Biology*. 1998b;24(3):427–442.